# Evaluation of Approaches for Calculating Warming Levels

Dr. Abby Lute
alute@woodwellclimate.org
*Last updated: July 21, 2023*

**Abstract**

Global warming levels are a useful shorthand for describing possible climate futures. Warming levels used by the Risk Team in the past span a variety of approaches but were poorly documented and represented only a subset of CMIP6 data. Here we develop a new table of yearly global mean surface temperatures for all CMIP6 data (models, members, scenarios) available from Google Cloud that can be used to experiment with alternative warming level calculation methods. We also evaluate different approaches of calculating and aggregating warming year data. Finally, we present new tables of warming years that span models, members, and scenarios and represent a much larger sample size than previous tables. These warming year tables, in combination with a suite of custom functions, can be used in future Risk Team analyses, particularly those focused on extreme values.

## 1. Introduction

Warming levels are defined as the amount of global temperature change since some baseline period (typically representing pre-industrial conditions) and are a simple way of quantifying the degree of climatic change. They are regularly used in policy and international climate negotiation contexts and are a useful shorthand for communicating climate change impacts. Some examples include the Paris Agreement setting the goal of keeping global warming well below 2°C relative to pre-industrial conditions (UNFCCC, 2015), and preferably below 1.5°C, and the Intergovernmental Panel on Climate Change (IPCC) special report on what a 1.5°C warmer world would look like (IPCC, 2018). Warming levels can provide a useful discussion framework since they may be more easily understood by nonscientific audiences and they avoid getting mired in discussions of timelines and scenarios and instead focus on the end result.

The Woodwell Climate Risk Team has used warming levels to communicate climate risks, for example in the maps for Probable Futures. The approach the Team has most often used is to find, for each global climate model (hereafter model), the first 21 year period when global mean surface temperature (GMST) exceeds the warming level of interest. Different climate metrics can then be calculated from these 21 years of data. The so-called warming years calculated using this approach are stored in the file monthly_models_thresholds_ssp585_v3.csv which is available upon request.

This approach is straightforward but has several drawbacks. First, the methods used to create the table are not well documented, making replication difficult to impossible. Second, the table only includes warming years for a small portion of the available models, ensemble members (also referred to as realizations), and scenarios available from CMIP6. Third, the use of the 21 year window and just a subset of CMIP6 runs limits the available sample size from which to assess extreme value statistics. Finally, the existing table is not conducive to experimentation with other methods of calculating warming levels as it only provides the final answer, not the intermediate data (i.e. GMST by year).

In the present work we aim to address these drawbacks. Our first objective is to create a comprehensive table of GMST for each year and each model, ensemble member, and scenario available from CMIP6. This will enable others to quickly experiment with different methods of calculating warming levels. Our second objective is to evaluate a few different approaches for calculating warming levels. This includes assessing the impacts of warming year aggregation methods on resulting warming levels. Finally, we develop new warming year tables that can be used in future work. Relevant code is available on GitHub at https://github.com/WoodwellRisk/Warming_levels and datasets are available upon request from the Woodwell Risk Team.

## 2. Previously used warming levels tables

There are three tables of warming levels that were previously used by the Risk Team. Each table provides warming years for 27 models, for SSP585, for the following warming levels: 1.0°C, 1.5°C, 2.0°C, 2.5°C, 3.0°C, 3.5°C, 4.0°C, and 4.5°C. It is unclear what ensemble members these data represent.

The warming year calculation methods for the three tables are described fully in the README and the code used to generate the tables is available in temperature_r_code_generate_CMIP6_year_temp_thresholds.R, both of which are available from the Risk Team. Here I briefly describe the three versions.

In the first table (monthly_models_thresholds_ssp585_v1.csv), the warming year is the first year in which GMST exceeds the warming level and does not drop below the warming level in subsequent years. This approach works fine for the SSP585 scenario considered in the table, but would not be useful for some warming levels when considering scenarios in which temperatures peak and then decline.

In the second table (monthly_models_thresholds_ssp585_v2.csv), the warming year is the first year in which GMST exceeds the warming level, regardless of temperatures in later years. This approach is sensitive to climatic variability, since one hot year could exceed the warming level long before this temperature is achieved on a regular basis.

In the third table (monthly_models_thresholds_ssp585_v3.csv), the warming year is the middle year of the first 21 year period when time-averaged GMST exceeds the warming level. When using this method in practice, there is the option of using all 21 years of the identified period instead of just using the middle year. This approach is similar to other rolling window approaches used in the literature (e.g. Seneviratne and Hauser, 2020).

## 3. New GMST Table

Recently, CMIP6 data has become available through Google Cloud in zarr format. This source offers many additional models, ensemble members, and scenarios than we currently have stored locally. We developed a new table of GMST (°K) for each available year from 1850 to 2150 and for each model, member, and scenario available from Google Cloud. Model/member combinations for which historical period data was not available were excluded. Additional CMIP6 data that has been flagged for errors is also available from Google Cloud but was not included in the GMST table. The table includes 1298 model/member/scenario combinations, compared to only 27 in the existing tables. The table also includes the 1850 through 1900 mean GMST, which is one way of quantifying pre-industrial temperature and can be used to calculate warming. The first few lines of the table are shown in Figure 1 and the full table is available upon request from the Risk Team. The GMST table should make calculating warming levels for different models/members/scenarios or using new methods relatively easy.

GMST was calculated from monthly surface air temperature (tas) from the CMIP6 models. Monthly tas was aggregated to annual tas using a weighted mean in which weights were based on the number of days in the month. Annual tas values were then averaged using a spatially weighted mean to arrive at GMST. The code used to calculate the GMST table is available in the GitHub repository (create_GMST_table_from_zarr_data.ipynb).

| | model | member | scenario | year | GMST | 1850-1900 |
|---|---|---|---|---|---|---|
| 0 | GFDL-CM4 | r1i1p1f1 | historical | 1850 | 285.901631 | 285.915908 |
| 1 | GFDL-CM4 | r1i1p1f1 | historical | 1851 | 286.032717 | 285.915908 |
| 2 | GFDL-CM4 | r1i1p1f1 | historical | 1852 | 286.029380 | 285.915908 |
| 3 | GFDL-CM4 | r1i1p1f1 | historical | 1853 | 286.068782 | 285.915908 |
| 4 | GFDL-CM4 | r1i1p1f1 | historical | 1854 | 286.109054 | 285.915908 |

Table 1. First 5 rows of the GMST table

As a check, we used the GMST table to recompute the warming years using the 21 year rolling mean approach used in the third table described above for the models and members we were able to identify the ensemble member for. One main difference is that the original table used locally stored CMIP6 data, whereas the newly computed table used CMIP6 data from Google Cloud. The difference in warming years between the old table and the new table is shown below. The identified warming years were the same for all models except for FGOALS-g3, for which the new warming years were 1 to 4 years later than the old warming years. The reasons for the differences in the FGOALS-g3 warming years are not clear. The overlap between historical and future scenarios in this model was accounted for in the new calculations, but it is not clear whether this was accounted for in the old table. It is hard to pin down the reason without knowing exactly which dataset the old warming years were calculated from.

| | Model | Yr1 | Yr1.5 | Yr2 | Yr2.5 | Yr3 | Yr3.5 | Yr4 | Yr4.5 |
|---|---|---|---|---|---|---|---|---|---|
| 0 | ACCESS-CM2 | 0 | 0.0 | 0.0 | 0.0 | 0.0 | 0.0 | 0.0 | 0.0 |
| 1 | ACCESS-ESM1-5 | 0 | 0.0 | 0.0 | 0.0 | 0.0 | 0.0 | 0.0 | 0.0 |
| 2 | CanESM5 | 0 | 0.0 | 0.0 | 0.0 | 0.0 | 0.0 | 0.0 | 0.0 |
| 4 | CNRM-CM6-1 | 0 | 0.0 | 0.0 | 0.0 | 0.0 | 0.0 | 0.0 | 0.0 |
| 5 | CNRM-CM6-1-HR | 0 | 0.0 | 0.0 | 0.0 | 0.0 | 0.0 | 0.0 | 0.0 |
| 6 | CNRM-ESM2-1 | 0 | 0.0 | 0.0 | 0.0 | 0.0 | 0.0 | 0.0 | 0.0 |
| 9 | EC-Earth3-Veg-LR | 0 | 0.0 | 0.0 | 0.0 | 0.0 | 0.0 | 0.0 | 0.0 |
| 10 | FGOALS-g3 | 2 | 4.0 | 1.0 | 2.0 | 2.0 | 2.0 | NaN | NaN |
| 11 | GFDL-CM4 | 0 | 0.0 | 0.0 | 0.0 | 0.0 | 0.0 | 0.0 | 0.0 |
| 15 | INM-CM4-8 | 0 | 0.0 | 0.0 | 0.0 | 0.0 | 0.0 | NaN | NaN |
| 16 | INM-CM5-0 | 0 | 0.0 | 0.0 | 0.0 | 0.0 | 0.0 | NaN | NaN |
| 17 | IPSL-CM6A-LR | 0 | 0.0 | 0.0 | 0.0 | 0.0 | 0.0 | 0.0 | 0.0 |
| 19 | MIROC6 | 0 | 0.0 | 0.0 | 0.0 | 0.0 | 0.0 | NaN | NaN |
| 20 | MIROC-ES2L | 0 | 0.0 | 0.0 | 0.0 | 0.0 | 0.0 | NaN | NaN |
| 21 | MPI-ESM1-2-HR | 0 | 0.0 | 0.0 | 0.0 | 0.0 | 0.0 | NaN | NaN |
| 22 | MPI-ESM1-2-LR | 0 | 0.0 | 0.0 | 0.0 | 0.0 | 0.0 | NaN | NaN |
| 23 | MRI-ESM2-0 | 0 | 0.0 | 0.0 | 0.0 | 0.0 | 0.0 | 0.0 | NaN |

Table 2. Difference in warming years (new minus old) between the newly calculated warming years based on Google Cloud data and the GMST table and the old warming years in monthly_models_thresholds_ssp585_v3.csv. Both new and old years were calculated using the 21 year moving window approach.

## 4. General approaches for calculating warming levels

There are several general approaches to calculating warming levels, some of which are outlined in James et al., (2017). Here we consider time sampling type approaches. The existing warming level tables fall under this category: first year to exceed the warming level, first year to exceed the warming level and not drop below it in subsequent years, and a temporal rolling mean approach.

An additional approach that we consider is a temperature window approach, which identifies years that are within some temperature range of the target warming level. This approach works for all scenarios, including overshoot scenarios, and is not overly sensitive to climatic variability. Although it is less common, this approach has been used for example by CSIRO to quantify warming levels (see here). They selected years within +/- 0.2°C of the target warming level as well as the five years before and after each of those years.

We used the GMST table to identify all years within +/- 0.25°C of the warming level. Compared to the 21 year moving window approach, this approach can result in a smaller or larger sample size. For example, when looking at SSP585 for the models and members used for a previous analysis called CERA, this approach identified between 7 and 27 years for each model for a warming level of 1°C and between 10 and 16 years for each model for a warming level of 2°C (Table 3) compared to the 21 years that would be identified using the 21 year moving window approach. For a 2°C warming level, the mean warming years from this approach were similar to those from the 21 year moving window approach (Table 3).

| | model | original_year | new_year | year_difference | nyears |
|---|---|---|---|---|---|
| 0 | ACCESS-CM2 | 2039 | 2037.5 | -1.5 | 10 |
| 1 | ACCESS-ESM1-5 | 2039 | 2039.5 | 0.5 | 14 |
| 2 | CNRM-CM6-1 | 2041 | 2039.0 | -2.0 | 11 |
| 3 | CNRM-CM6-1-HR | 2030 | 2030.5 | 0.5 | 10 |
| 4 | CNRM-ESM2-1 | 2046 | 2045.0 | -1.0 | 13 |
| 5 | CanESM5 | 2023 | 2022.5 | -0.5 | 12 |
| 6 | EC-Earth3-Veg-LR | 2042 | 2041.5 | -0.5 | 12 |
| 7 | FGOALS-g3 | 2046 | 2046.5 | 0.5 | 10 |
| 8 | GFDL-CM4 | 2042 | 2042.5 | 0.5 | 10 |
| 9 | INM-CM4-8 | 2046 | 2046.0 | 0.0 | 13 |
| 10 | INM-CM5-0 | 2046 | 2044.5 | -1.5 | 16 |
| 11 | IPSL-CM6A-LR | 2034 | 2034.0 | 0.0 | 11 |
| 12 | MIROC-ES2L | 2047 | 2047.5 | 0.5 | 10 |
| 13 | MIROC6 | 2053 | 2053.5 | 0.5 | 12 |
| 14 | MPI-ESM1-2-HR | 2049 | 2048.5 | -0.5 | 12 |
| 15 | MPI-ESM1-2-LR | 2049 | 2048.5 | -0.5 | 16 |
| 16 | MRI-ESM2-0 | 2038 | 2038.5 | 0.5 | 10 |

Table 3. Comparison of warming years from different approaches for the 17 model/member combinations used in CERA for SSP585 for a 2°C warming level. The ‘original year’ column shows the warming year from the existing table that uses the 21 year moving window approach (monthly_models_thresholds_ssp585_v3.csv). The ‘new year’ column shows the mean warming year calculated using the temperature window approach (all years with warming between 1.75°C and 2.25°C). The ‘year difference’ column shows the difference between the two warming years. The ‘nyears’ column shows the number of years used in the ‘new year’ calculation.

## 5. Aggregation approaches

Aggregation of warming years across models, ensemble members, or scenarios has been suggested as a way to both increase sample size and account for uncertainty associated with models, natural variability, and emissions pathways, respectively. Aggregation of model outputs across multiple models (often referred to as the multi-model mean or ensemble mean) is a common practice in climate science that has been shown to reduce bias relative to using individual models (Tebaldi and Knutti, 2007). Aggregation across ensemble members, particularly those reflecting different initial conditions, can be helpful to mute the effects of natural internal climate variability (Deser et al., 2020). This may be particularly important when using warming year calculation methods such as that used in monthly_models_thresholds_ssp585_v2.csv (the warming year is the first year exceeding the warming level).

Unlike aggregating across models or ensemble members, the concept of aggregating warming years, or climate outputs more generally, across scenarios has more limited precedent in the scientific literature. Therefore, we investigated this idea in more detail.

### 5.1 Aggregation across scenarios

As discussed in James et al., (2017), regional responses to a specific warming level might vary with scenario "if regional change is sensitive to the rate of warming, lags in the climate system, emissions reductions, or temperature overshoot." Lags in the climate system are a relevant consideration for glaciers, ice sheets, and sea level, as well as the elements that closely depend on them, which might include regional temperature and precipitation. Periods during which $CO_2$ is increasing and during which $CO_2$ is decreasing may have the same GMST but with regional contrasts (see citations in James et al., 2017). Finally, the higher temperatures achieved in overshoot scenarios may entail irreversible changes in some elements that would not be present in other scenarios at the same warming level (see citations in James et al., 2017)

Pendergrass et al., (2015) show that the amount of mean precipitation change per degree of global warming does depend on emission scenario, with greater change found in lower emissions scenarios (see their Figure 2a; see also Caesar et al., 2013). In contrast, they show that the amount of change in extreme precipitation per degree warming is indistinguishable across emissions scenarios (see their Figure 2b).

Tebaldi et al., (2021) present maps of normalized temperature and precipitation changes (section 3.1.2, Figure 2) for a suite of models and scenarios. The normalized changes are calculated as the change in temperature or precipitation between the end of the 21st century and the historical baseline, divided by the change in GMST. They show that intermodel variability exceeds interscenario variability for both temperature and precipitation (their Figure 2e-h), although they mention that internal variability could be contributing more to the intermodel variability than to the interscenario variability.

Seneviratne and Hauser (2020) aggregate warming levels across scenarios in their comparison of climate extremes from CMIP5 and CMIP6. They show that differences in annual hottest daytime temperature anomalies at different warming levels based on just SSP585 and based on the combination of SSP119, SSP126, SSP245, and SSP370 are nonsignificant (see their Section 3.1 and Figure S4). They do caution against using all available ensemble members from each model however due to concerns about uneven model weighting (see their Section 3.1 and Figure S5).

Seneviratne et al., (2016) show that changes in temperature and precipitation extremes scale with global warming with little difference between RCP4.5 and RCP8.5. Wartenburger et al., (2017) built on this to show that for CMIP5 changes in many climate indices (related to temperature, precipitation, drought, etc) scale well with global warming regardless of scenario (they considered RCP2.6, RCP4.5, RCP6.0, and RCP8.5; see their Figures 3 and 4).

Working Group 1 of the latest IPCC Assessment Report discusses this issue at some length (IPCC AR6 WG1, Chapter 11, Cross-Chapter Box 11.1, pages 1542-1546, cited as Seneviratne et al., 2021). Based on the latest literature they conclude that the climate response to a given warming level is consistent across scenarios for many climate variables. They note greater consistency for temperature related variables than for those related to hydrology or atmospheric dynamics, and lower consistency for low emissions scenarios than other scenarios. They also note that even for a pathway dependent variable such as mean precipitation (e.g. Pendergrass et al., 2015), model uncertainty and internal variability are larger than scenario uncertainty for a given warming level. In Figure 3 of Cross-Chapter Box 11.1 they provide an example of warming level maps in which data was aggregated across models and scenarios. However, they emphasize that using scenarios (as opposed to warming levels) is important for variables that a) depend on radiative forcings such as aerosols or land use and land management, b) are time or warming rate dependent (as discussed above), or c) differ between transient and equilibrium states. They also caution that climate response at a given warming level in overshoot scenarios may differ before and after overshoot.

Many studies which aggregate across scenarios use warming years calculated from a moving window approach. CSIRO used a temperature window approach (https://www.climatechangeinaustralia.gov.au/en/changing-climate/future-climate-scenarios/global-warming-levels/) and mentioned that warming years can be aggregated across scenarios (https://www.climatechangeinaustralia.gov.au/media/ccia/2.2/cms_page_media/585/Technical%20Note%203%20-%20Global%20Warming%20Levels%20methods_1.pdf), although in the end they chose to use a single scenario.

Based on the literature presented above, the overarching impression is that aggregating across scenarios is acceptable and useful when variables are pathway (i.e. scenario) independent, but not when variables are pathway dependent. This raises the question of how to define pathway dependence and how much pathway dependence is too much. Some of the papers above identified particular variables as being pathway dependent or independent. Identified pathway dependent variables include global mean precipitation (although perhaps not regional mean precipitation, see IPCC citation), slow responding elements of the cryosphere (glaciers, ice sheets), and sea level rise. Pathway independent variables include temperature related variables, temperature and precipitation extremes, quick responding elements of the cryosphere (sea ice area, permafrost, snow), some drought metrics, and soil moisture.

### 5.1.1 Comparison of temperature change across scenarios

We investigated differences in warming across scenarios for a given warming level by first plotting maps of warming for each scenario in a 2°C world (Figure 1), as determined by the temperature window approach (i.e. all years within +/-0.25°C of 2°C warming). We note that the fact that warming levels may look different under different scenarios does not necessarily invalidate the idea of aggregating across scenarios.

In order to provide the most direct comparison across scenarios, we only used model/member combinations that provided data for the full 2015-2099 period and had data for all 8 scenarios. Unfortunately, this restricted the analysis to one model (CNRM-ESM2-1) and five members. Broad scale patterns of warming were consistent across scenarios; the Arctic experienced much greater warming than other areas and land areas typically saw more warming than oceans (Figure 1).

Using the same data, we calculated the range of warming at each grid location (warmest scenario at that grid cell minus coldest scenario at that grid cell; Figure 2). The largest ranges of warming (on the order of 1.5°C) were found in polar ocean regions, which may be due to uncertainty in future sea ice extent as described in Tebaldi et al., (2021). The range of warming over land areas was mostly less than 0.9°C.

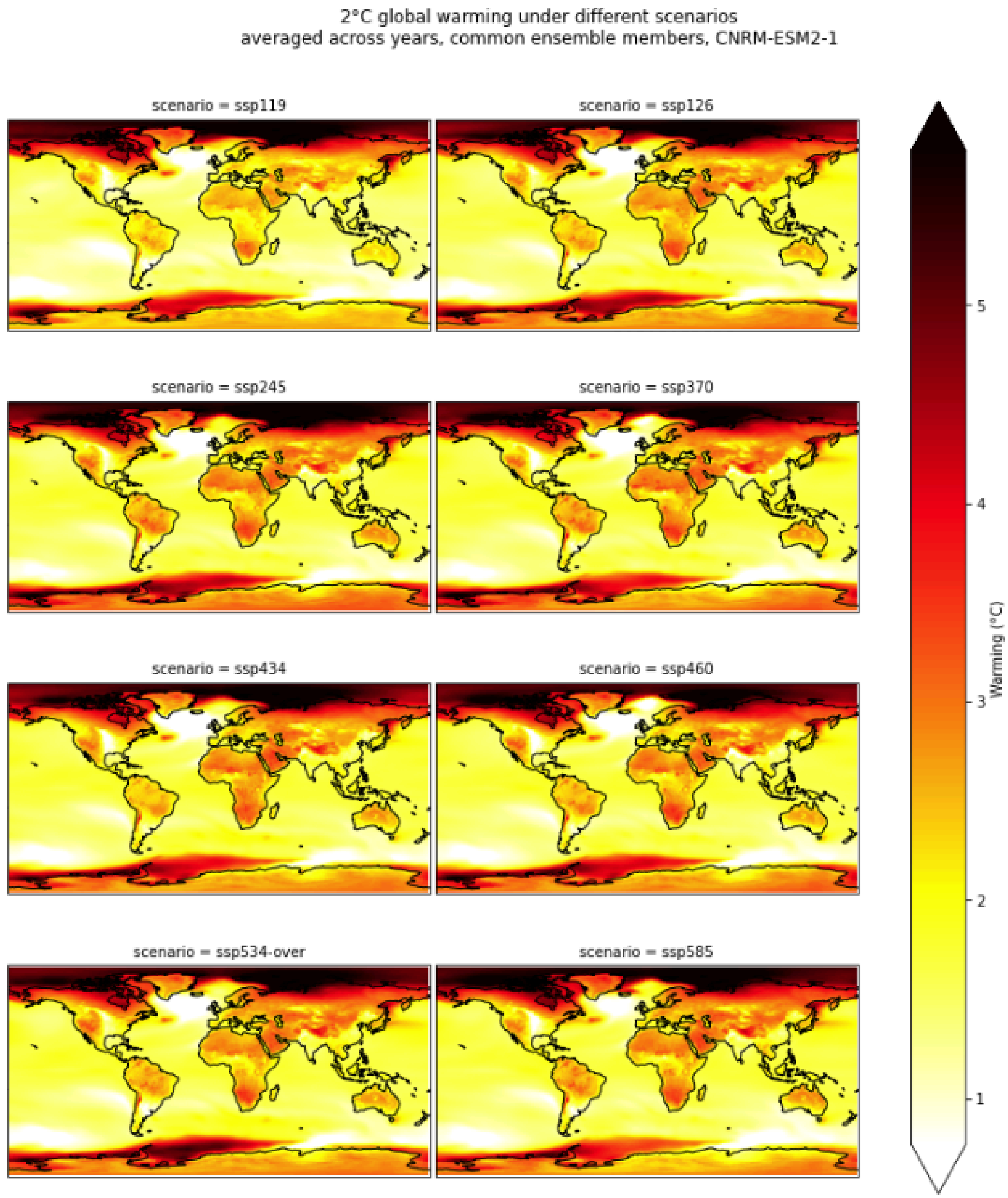


Figure 1. Warming in a 2°C world under different scenarios. Calculations are based only on the model (n=1) and members (n=5) all scenarios had in common and used a temperature window approach to warming year identification.

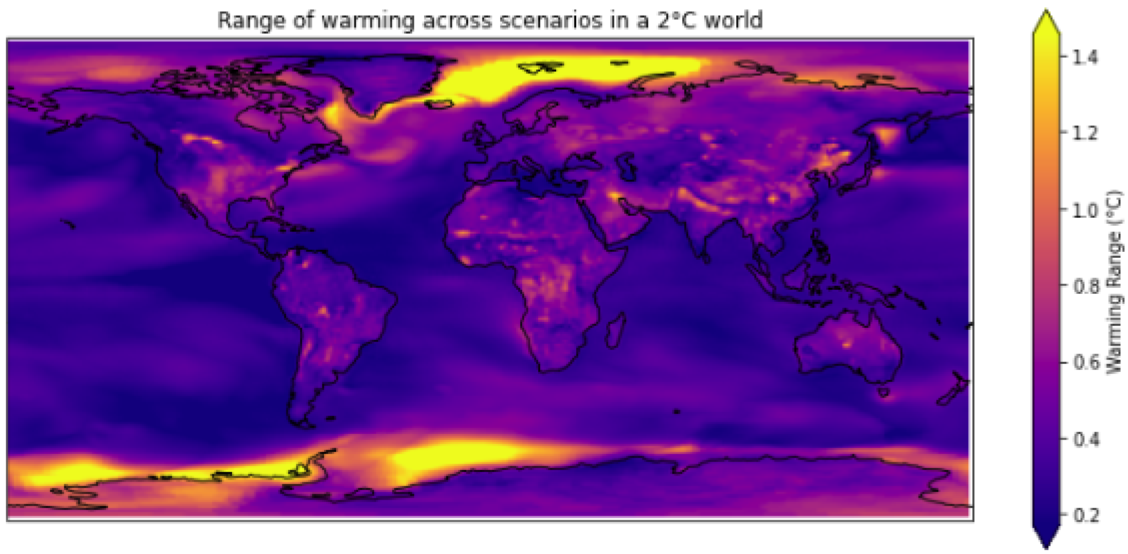


Figure 2. Range (max minus min) of warming across scenarios in a 2°C world.

Using a leave-one-out experiment, SSP119 was found to be the scenario contributing the most to global mean spread in warming in a 2°C world (Figure 3). This was further supported by Figure 4, which shows the difference in warming in a 2°C world between each pair of scenarios. SSP119 again stands out as having the largest contrasts with other scenarios, reaching 1°C in some locations. The differences amongst the other scenarios were typically within +/- 0.25°C, especially over land areas.

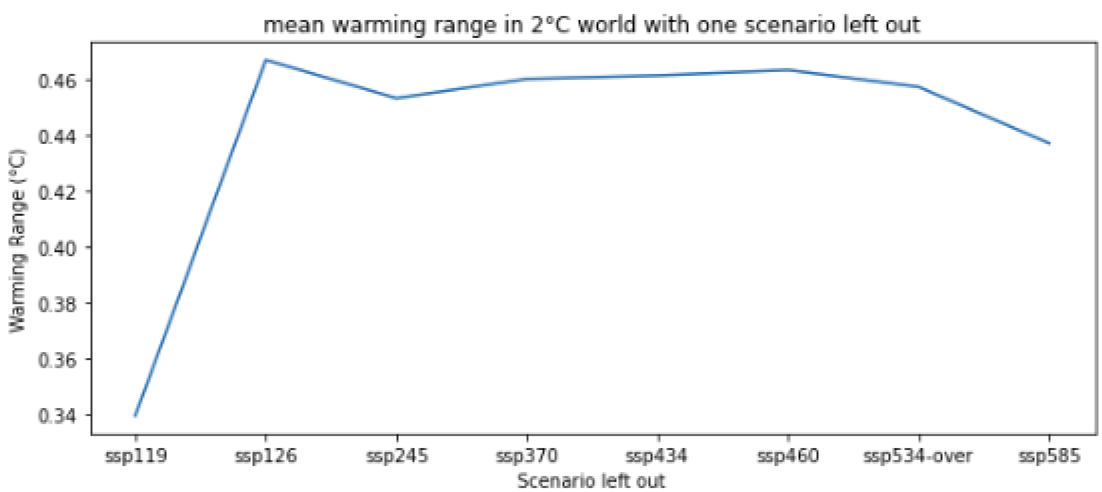


Figure 3. Range (max minus min) of warming across scenarios in a 2°C world with the scenario indicated on the x-axis left out. Lower y values indicate that leaving that scenario out reduced the scenario spread in warming.

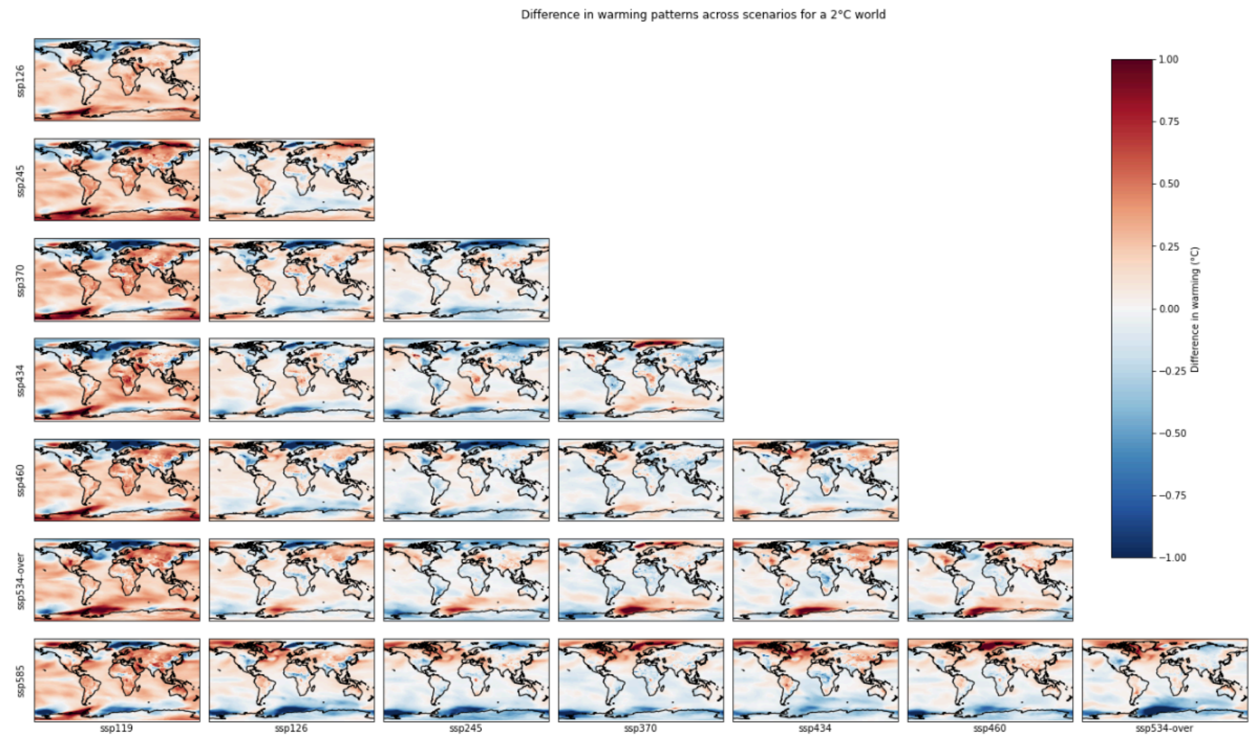


Figure 4. Difference in warming in a 2°C world for each pair of scenarios using the temperature window approach. All scenarios use the same model and 5 members.

A brief comparison of warming across scenarios using the 21 year moving window approach is shown in Figure 5. For this the same model and 5 ensemble members were used. The SSP119 scenario did not reach a 2°C warming level in any of the ensemble members and is therefore excluded. The SSP126 scenario only reached 2°C in 3 of the 5 scenarios, so some of the contrasts shown in Figure 5 can be attributed to the different ensemble used for SSP126 compared to the other scenarios.

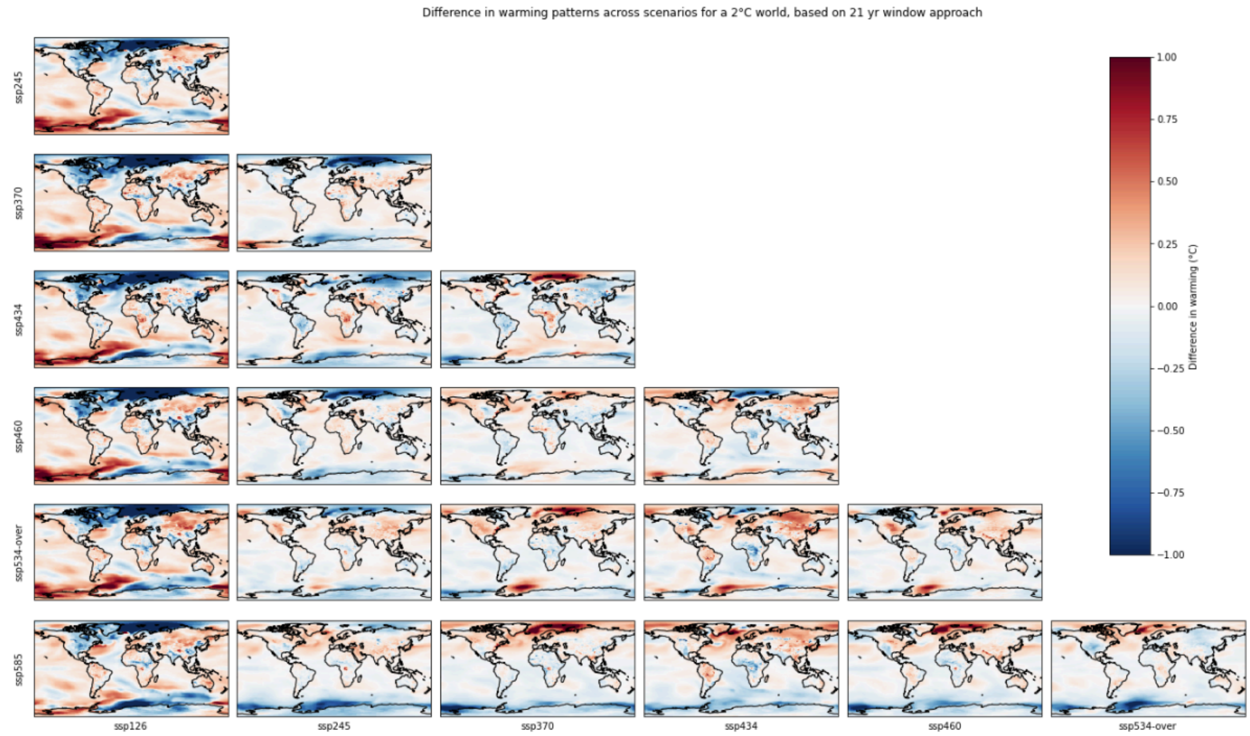


Figure 5. Difference in warming in a 2°C world for each pair of scenarios using the 21 year moving window approach. All scenarios use the same model and 5 members, except SSP126 for which only 3 members reached 2°C.

##### 5.1.1.1 Comparison of temperature standard deviation and 95th percentile across scenarios

We further investigated differences in temperature across scenarios for a given warming level by comparing the temperature standard deviation and 95th percentile under SSP245, SSP370, and SSP585. For this analysis, warming levels were defined using the 21 year moving window approach and the best subset of model/member/scenario combinations (described in section 6.1) which only includes one member per model. Only models that were available for both scenarios were included in the comparisons. For each scenario and warming level combination, the standard deviation of annual temperature was computed across models and the 21 years. The 95th percentile of annual temperature was calculated similarly. We considered warming levels of 1°C, 2°C, and 3°C.

Broad scale patterns of temperature standard deviation were similar across scenarios and warming levels. The lowest standard deviations (<1°C) were found over oceans outside of polar regions whereas the highest standard deviations (>4°C) were found in the coldest locations- the Arctic, Antarctica and surrounding oceans, the Tibetan Plateau, and the Andes. Differences in temperature standard deviation between the two scenarios were less than 0.2°C in almost all locations for all three warming levels. Plots are shown below for the case of a 2°C warming level (Figures 6 and 7).

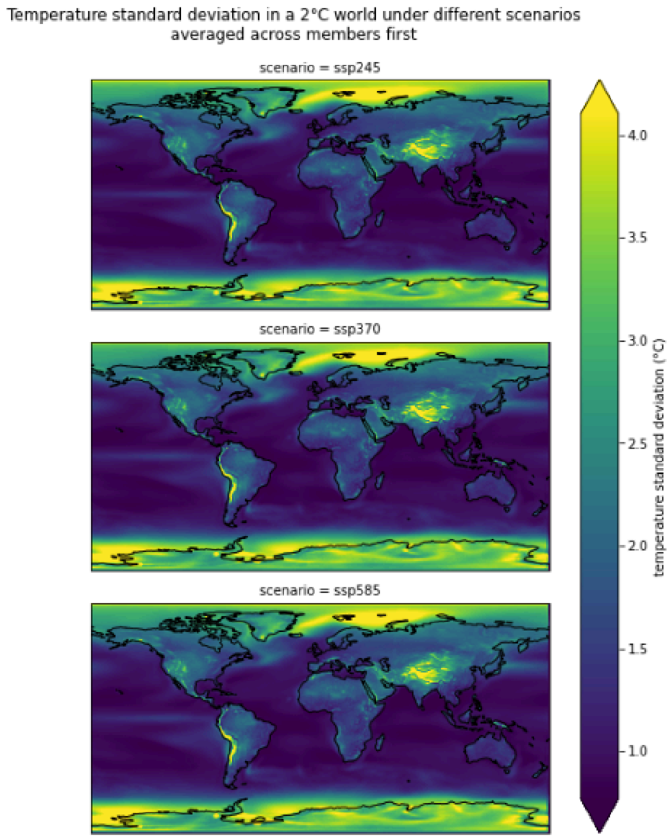


Figure 6. Standard deviation of annual temperature in a +2°C world under SSP245 (top), SSP370 (middle) and SSP585 (bottom).

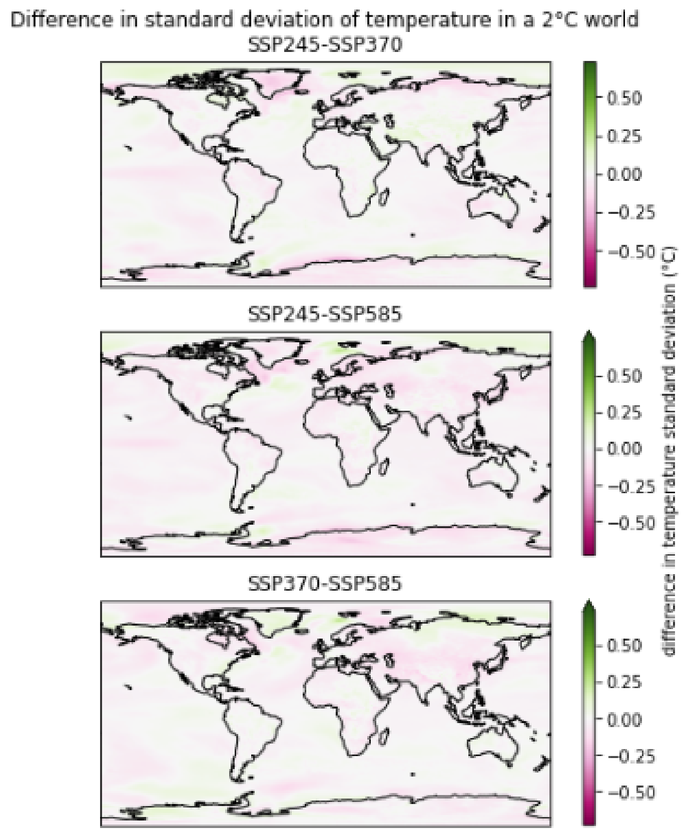


Figure 7. Difference between scenarios in the standard deviation of annual temperature in a +2°C world.

The global range of 95th percentile temperatures spans more than 80°C. In most locations and warming levels, the difference in 95th percentile temperature between the scenarios is less than 1°C. The largest differences were located in polar regions. Plots are shown below for the case of the 2°C warming level (Figure 8 and 9).

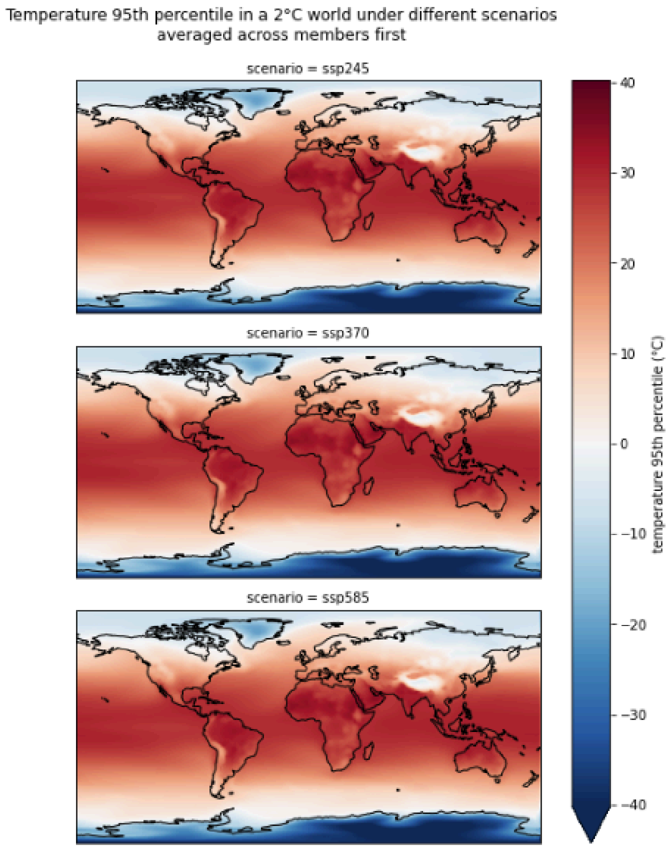


Figure 8. 95th percentile of annual temperatures in a +2°C world under SSP245 (top), SSP370 (middle), and SSP585 (bottom).

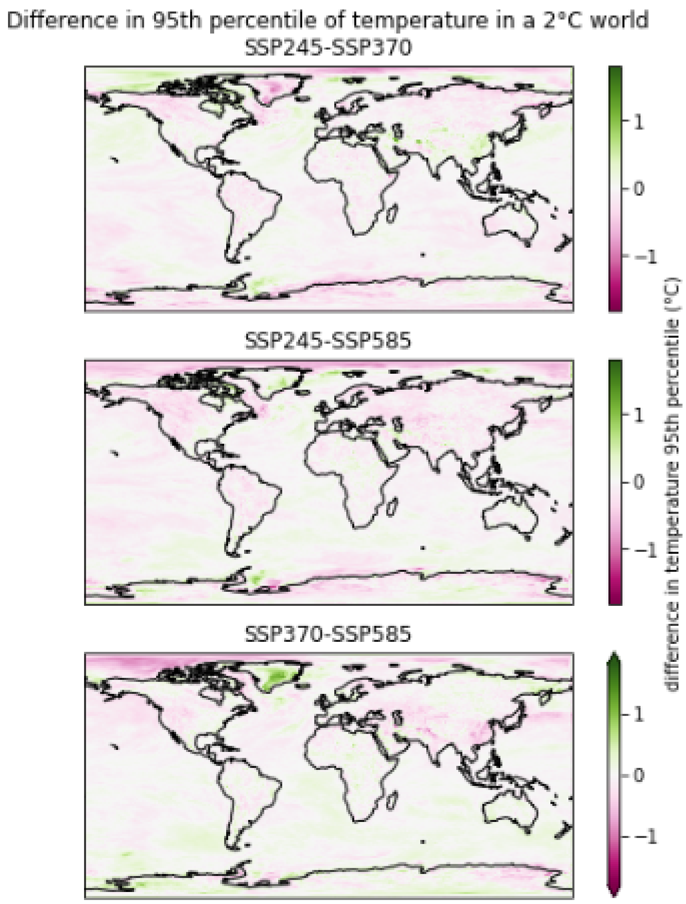


Figure 9. Difference between scenarios in the 95th percentile of annual temperatures in a +2°C world.

### 5.1.2 Comparison of precipitation change across scenarios

As with warming, we investigated differences in precipitation change across scenarios for a given warming level by first plotting maps of warming for each scenario in a 2°C world (Figure 10). We used the same warming years (based on the temperature window approach), ensemble members, and model as above. Spatial patterns of annual precipitation were similar across scenarios.

Using the same data, we calculated the absolute and percent range of annual precipitation at each grid location (Figure 11). The absolute range was calculated as the wettest scenario at that grid cell minus driest scenario at that grid cell. The percent range was calculated as the absolute range divided by the scenario-mean. The largest absolute ranges of annual precipitation (greater than 250 mm) were found over equatorial oceans. The largest percent ranges of annual precipitation (greater than 30%) were found over the equatorial Pacific and over areas with low annual precipitation such as N Africa and the Middle East. The range of precipitation over land was typically less than 170 mm or 30%.

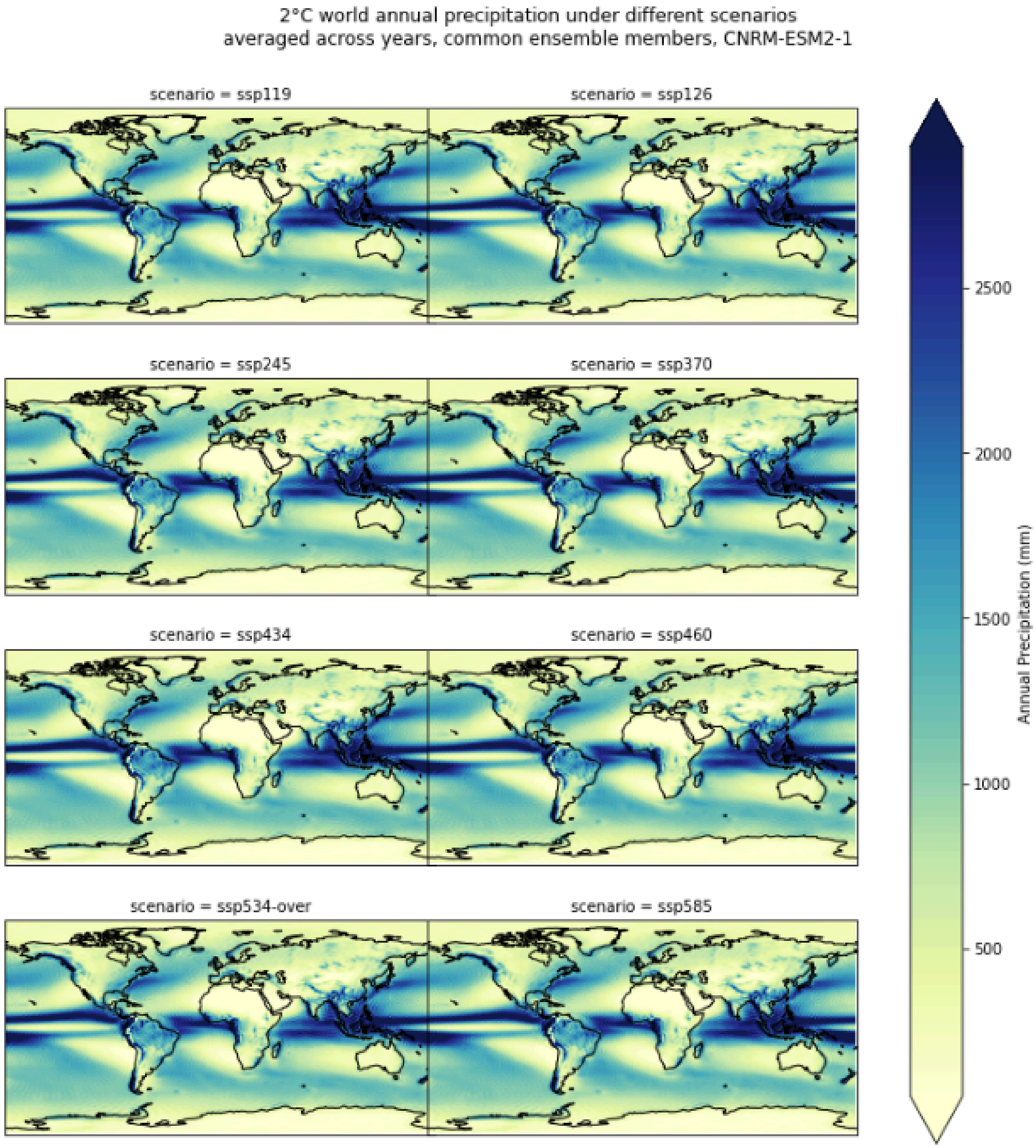


Figure 10. Annual precipitation in a 2°C world under different scenarios. Calculations are based only on the model (n=1) and members (n=5) all scenarios had in common and used a temperature window approach to warming year identification.

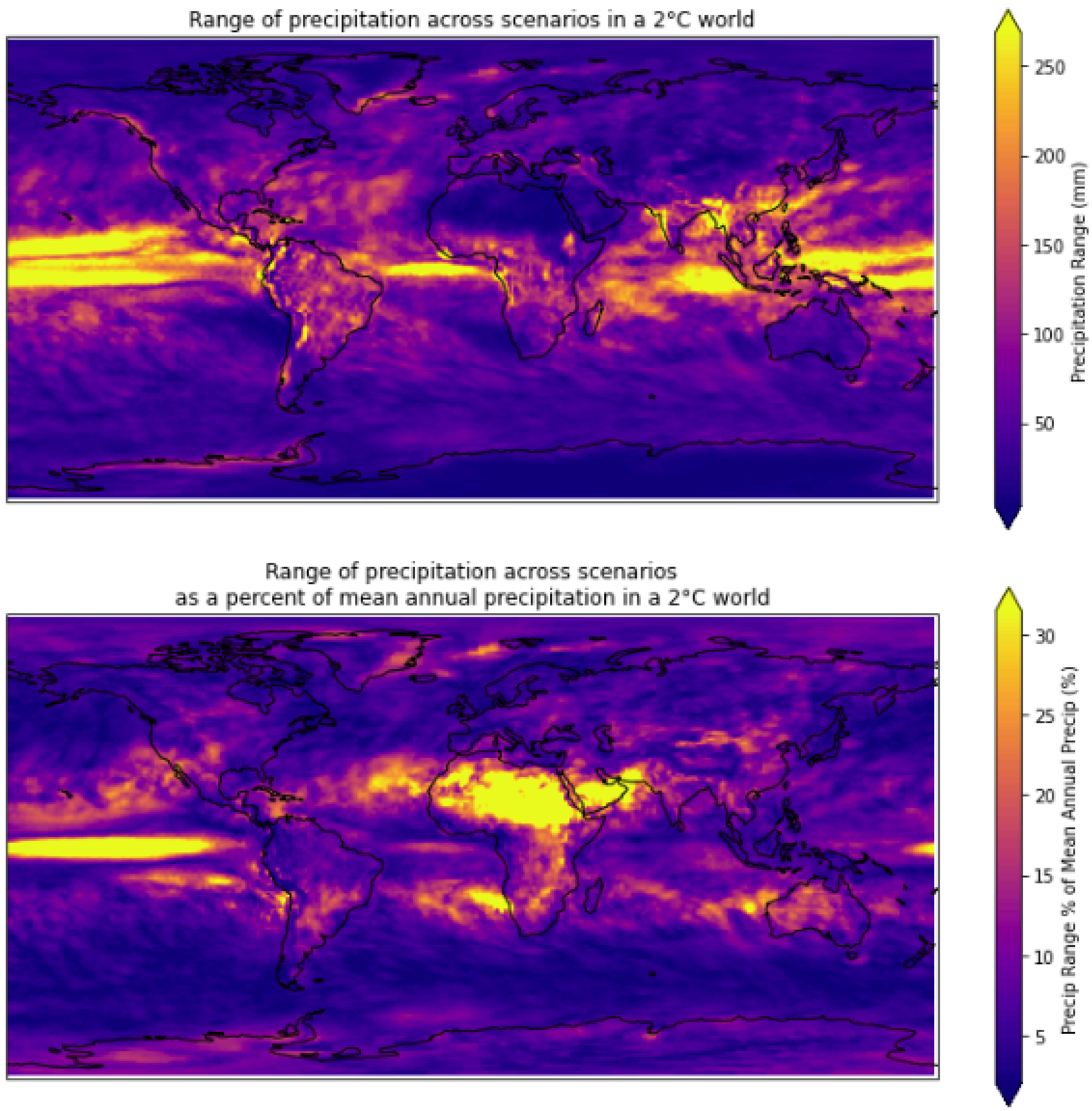


Figure 11. Range of annual precipitation across scenarios in a 2°C world. (Top) Absolute range (max minus min). (Bottom) Percent range ((max minus min) divided by the scenario-mean).

As with temperature, we evaluated which scenarios contributed most to the spread in precipitation (Figure 12). Again, SSP119 was the biggest contributor. Leaving out this scenario reduced the global mean absolute precipitation range by almost 20%.

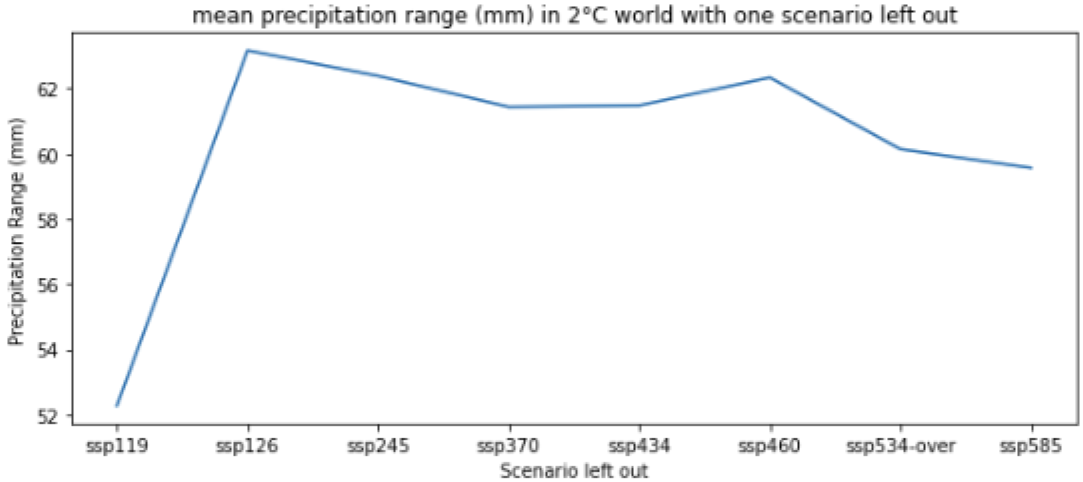


Figure 12. Range (max minus min) of warming across scenarios in a 2°C world with the scenario indicated on the x-axis left out. Lower y values indicate that leaving that scenario out reduced the scenario spread in precipitation.

Plots comparing annual precipitation for each pair of scenarios supported the conclusion that SSP119 had the largest contrasts with other scenarios (Figures 13 and 14). Amongst other scenarios differences were small, especially over land areas (typically less than +/-75 mm or +/-10%).


Figure 13. Difference in annual precipitation in a 2°C world (max minus min) for each pair of scenarios using the temperature window approach.

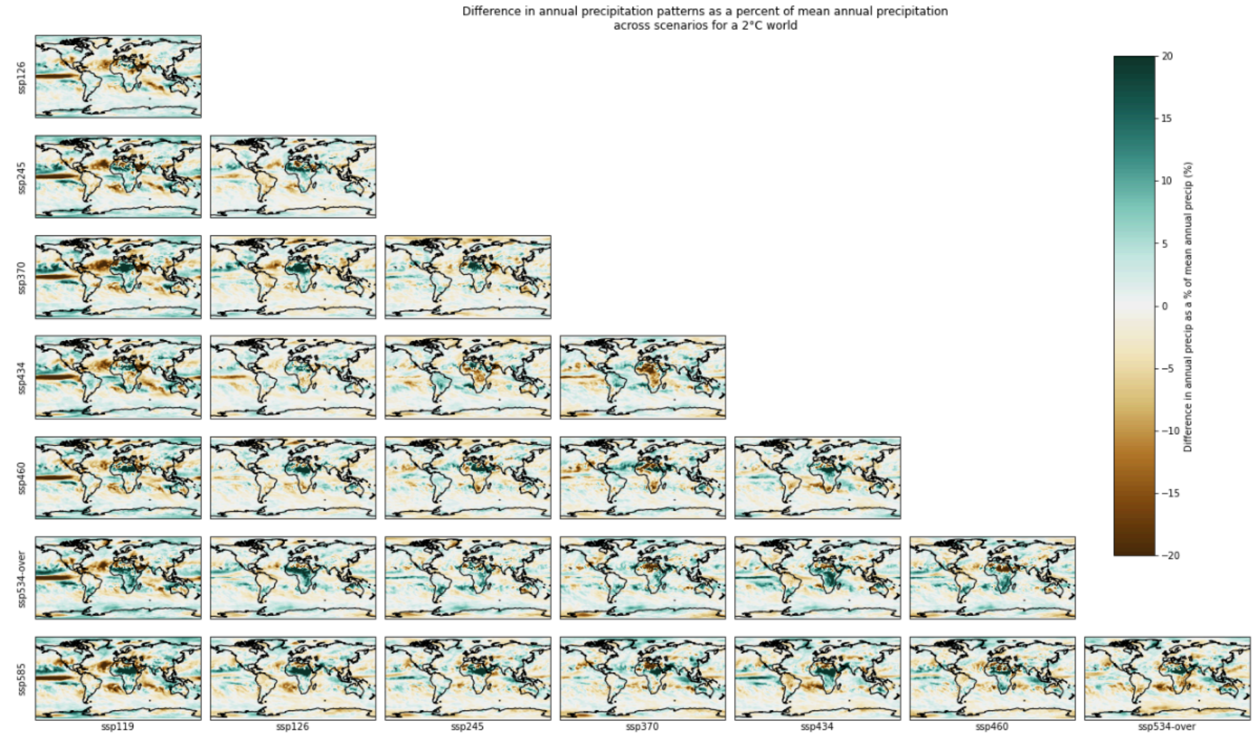


Figure 14. Percent difference in annual precipitation in a 2°C world (max minus min divided by the all scenario mean) for each pair of scenarios using the temperature window approach.

The previous plots were replicated using the 21 year moving window approach to calculating warming years (Figures 15 and 16). The absolute and percent differences in precipitation between scenarios were broadly similar to those using the temperature window approach. Differences for SSP126 were slightly larger due to the difference in ensemble size.

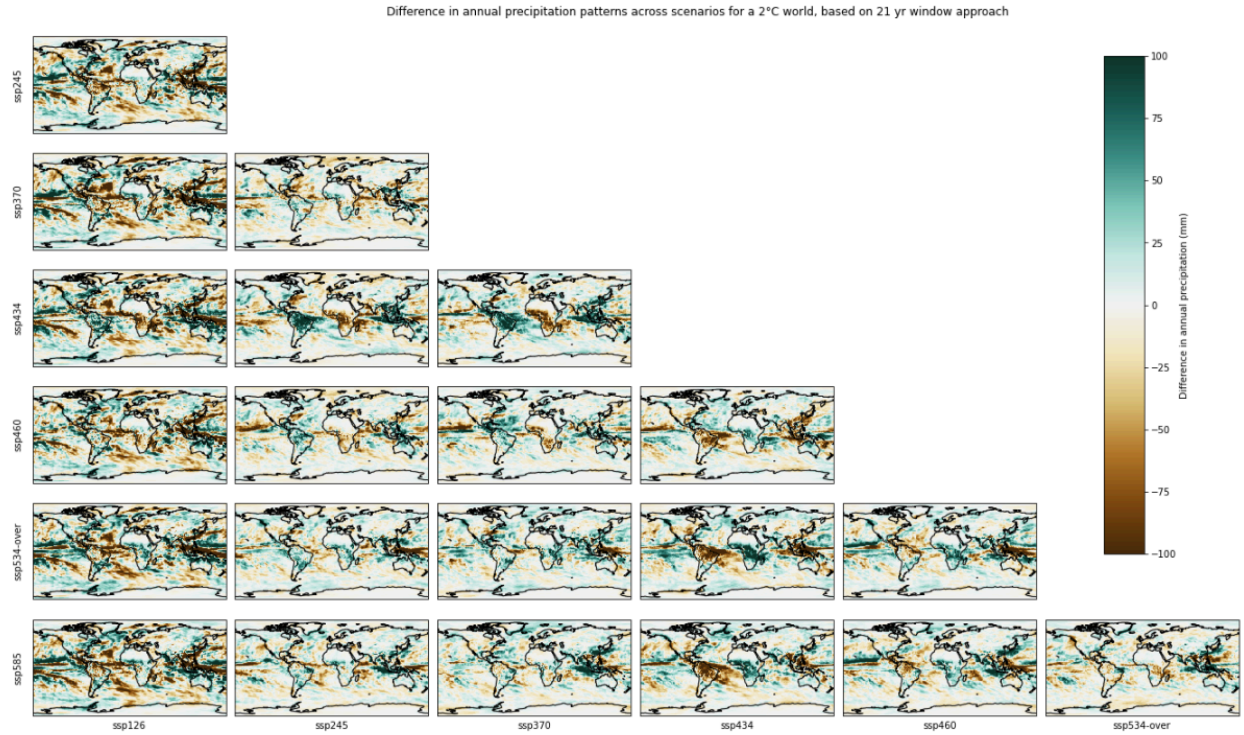


Figure 15. Difference in annual precipitation in a 2°C world (max minus min) for each pair of scenarios using the 21 year window approach. All scenarios use the same model and 5 members, except SSP126 for which only 3 members reached 2°C.

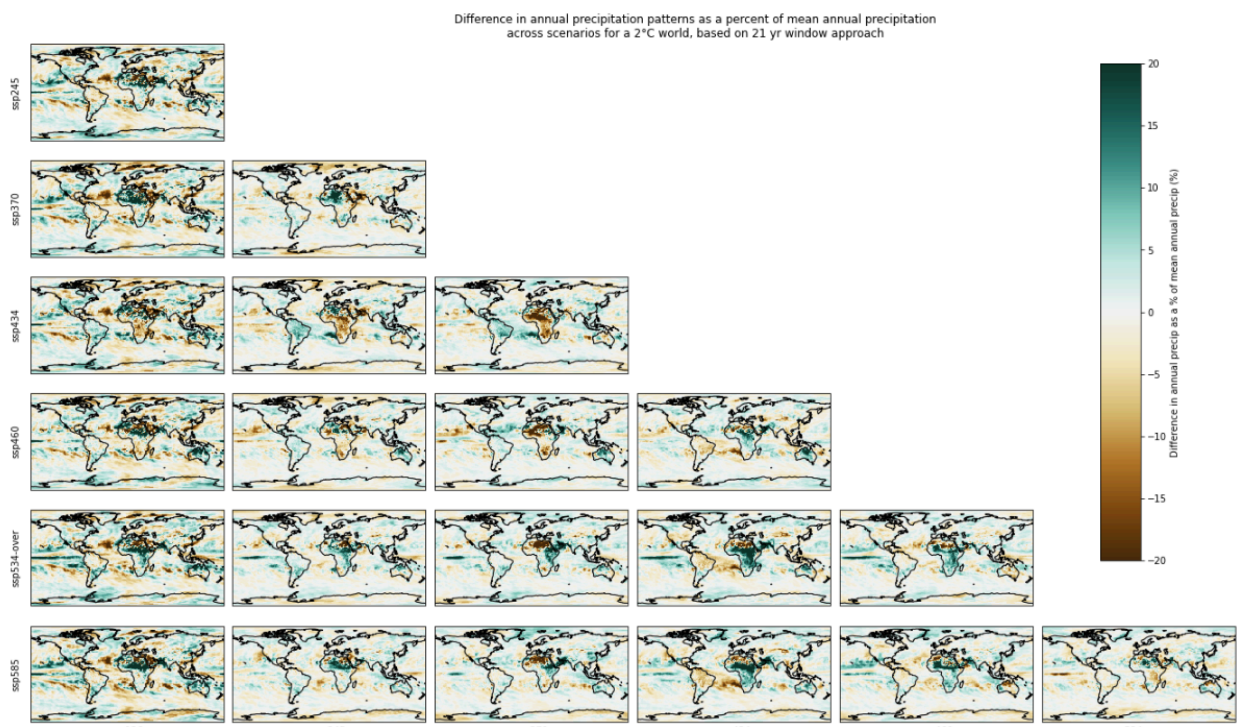

Figure 16. Percent difference in annual precipitation in a 2°C world (max minus min divided by the all scenario mean) for each pair of scenarios using the 21 year window approach. All scenarios use the same model and 5 members, except SSP126 for which only 3 members reached 2°C.

#### 5.1.2.1 Comparison of annual precipitation standard deviation and 95th percentile across scenarios

We further investigated differences in precipitation across scenarios for a given warming level by comparing the standard deviation and 95th percentile of annual precipitation under SSP245, SSP370, and SSP585. For this analysis, warming levels were defined using the 21 year moving window approach and the best subset of model/member/scenario combinations (described in section 6.1) which only includes one member per model. Only models that were available for both scenarios were included in the comparisons. For each scenario and warming level combination, the standard deviation of annual precipitation was computed across models and the 21 years. The 95th percentile of annual precipitation was calculated similarly. We considered warming levels of 1°C, 2°C, and 3°C.

Broad scale patterns of annual precipitation standard deviation were similar across scenarios and warming levels. The spatial pattern of precipitation standard deviation was similar to the spatial pattern of precipitation- the smallest standard deviations were generally found in drier areas and the largest standard deviations (in excess of 800 mm) were found in the tropics and large mountain ranges. Across warming levels, the difference in precipitation standard deviation was less than 10% of the scenario/model/year mean annual precipitation in almost all locations. Plots are shown below for the case of the 2°C warming level (Figures 17 and 18).

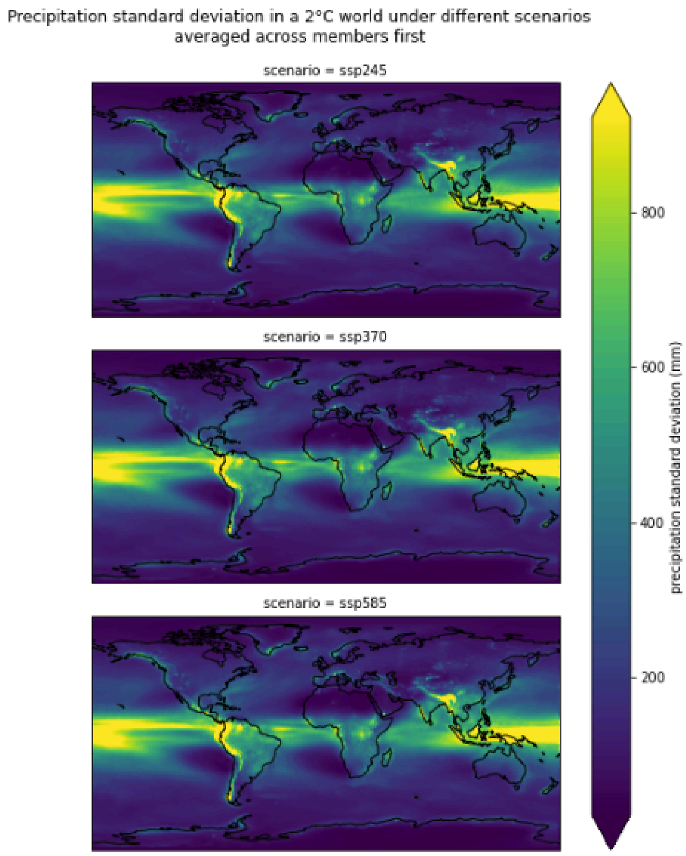


Figure 17. Standard deviation of annual precipitation in a +2°C world under SSP245 (top), SSP370 (middle), and SSP585 (bottom).

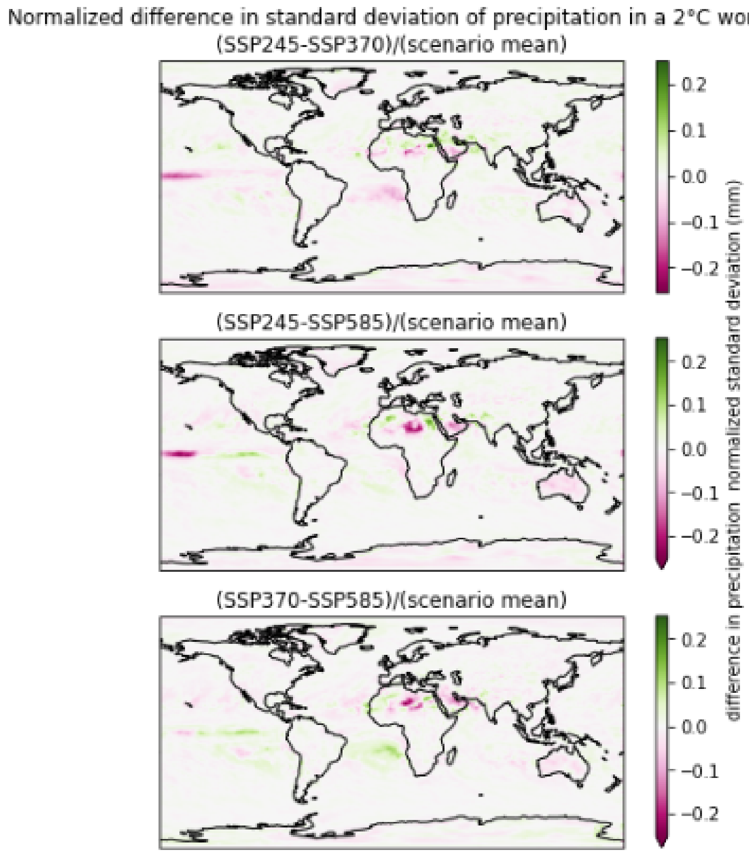


Figure 18. Normalized difference between scenarios in the standard deviation of annual precipitation in a +2°C world. Normalized difference was computed as the difference between the two specified scenarios divided by the scenario-mean annual precipitation.

Spatial patterns of the 95th percentile of annual precipitation were very similar across scenarios and warming levels. Differences across scenarios in 95th percentile precipitation were typically less than 20% of the scenario/model/year mean annual precipitation, but did exceed 50% in some cases. Plots are shown below for the case of the 2°C warming level (Figure 19 and 20).

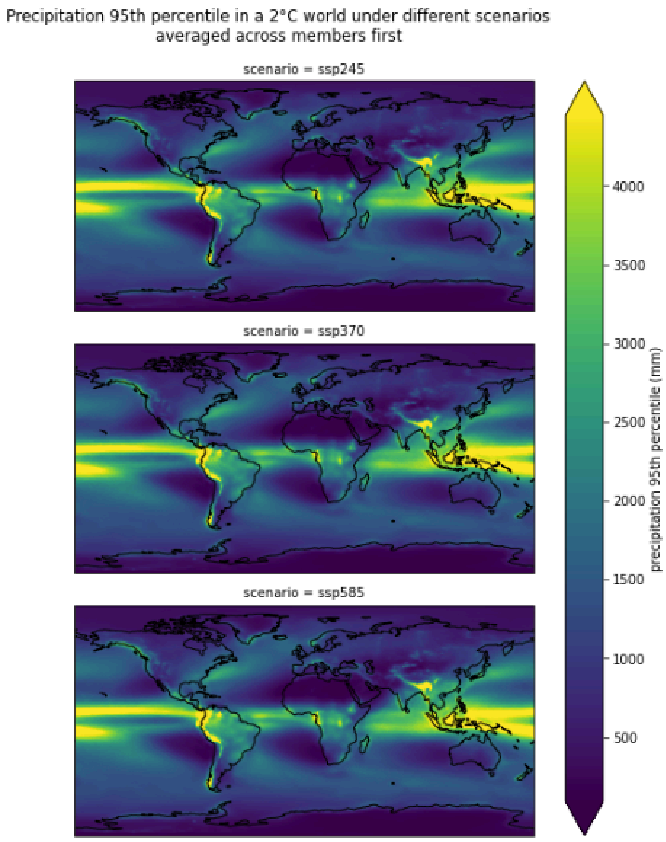


Figure 19. 95th percentile of annual precipitation in a +2°C world under SSP245 (top), SSP370 (middle), and SSP585 (bottom).

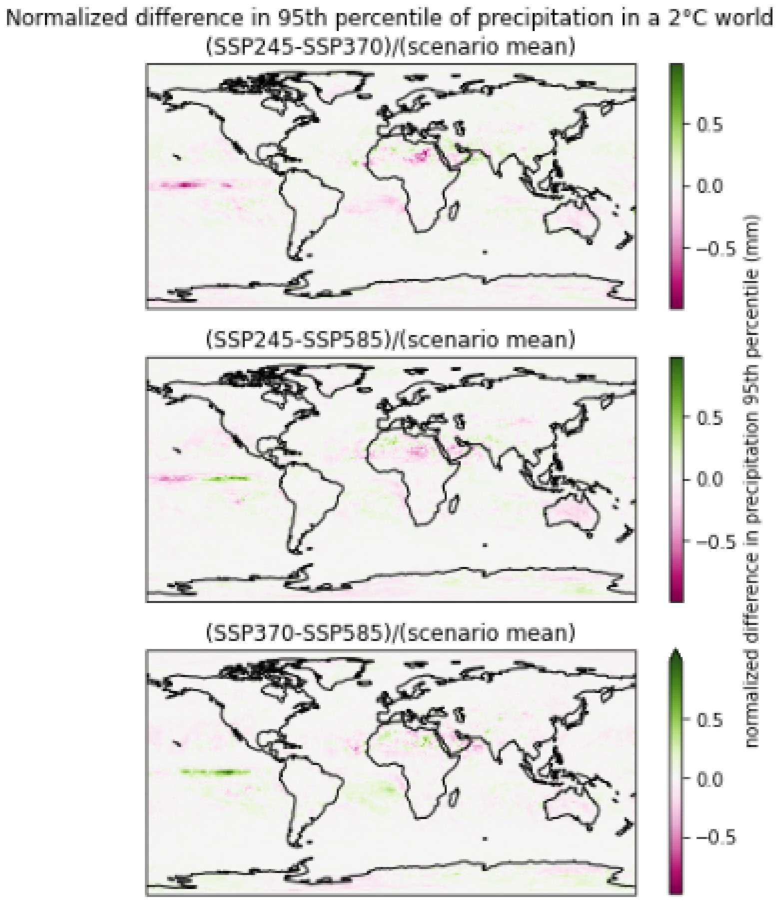


Figure 20. Normalized difference between scenarios in the 95th percentile of annual precipitation in a +2°C world. Normalized difference was computed as the difference between the two specified scenarios divided by the scenario-mean annual precipitation.

### 5.2 Data availability considerations with respect to aggregation

Based on the literature review and analyses above, it appears appropriate to aggregate warming levels across models, members, and/or scenarios, with a few caveats.

The first caveat concerns pathway dependence of the variable under consideration. As discussed above, aggregation across scenarios is only appropriate for pathway independent variables (see section 5.1 for further details on this and examples of pathway dependent and pathway independent variables).

The second caveat concerns weighting. Several authors have indicated that when considering aggregating across models, ensemble members, and/or scenarios it is important that equal weighting is given (e.g. Seneviratne and Hauser (2020)). For example, some models were only run for a subset of scenarios, so if all model/scenario combinations were included and given equal weight then some scenarios would be represented by fewer data points and thus be less heavily weighted. A similar concern applies to the number of ensemble members available for each model.

Figure 21 shows the availability of models for each scenario, restricted to those that provide data for the full future time period (2015-2099) in the case of future scenarios. If all models and all scenarios were used with equal weight there would be a lot more data points for some scenarios than for others. Only two models provide data for every scenario, whereas 37 models provide data for the historical and all tier 1 scenarios (SSP126, SSP245, SSP370, and SSP585).

Figure 22 shows the availability of members for each model. Some models have a much larger number of ensemble members available (e.g. ACCESS-ESM1-5). It is also clear that some ensemble members are available from a larger number of models, however ensemble members are defined differently for each model, so it is meaningless to restrict the ensemble members to a particular label (e.g. r1i1p1f1).

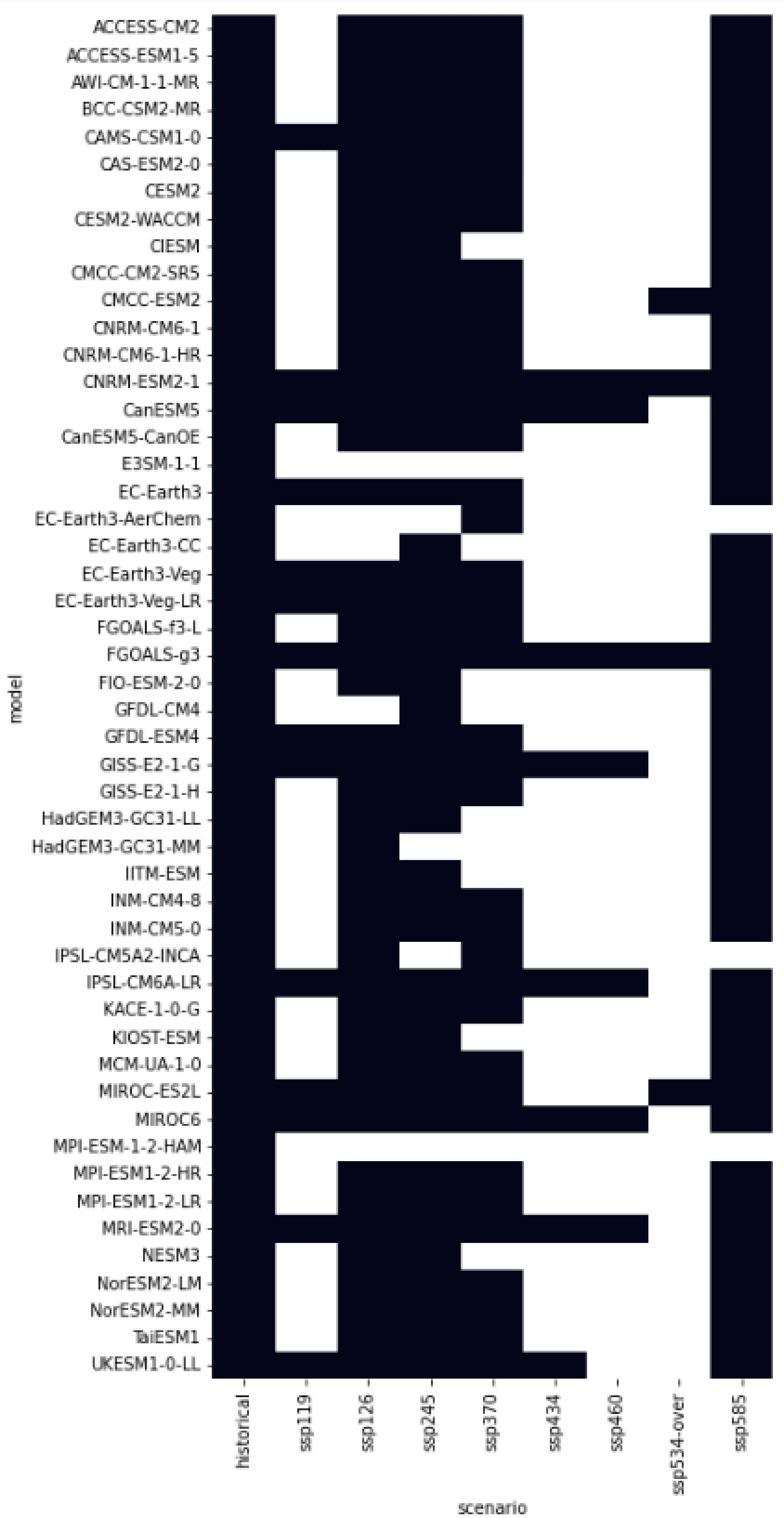


Figure 21. CMIP6 model/scenario availability based on Google Cloud data.

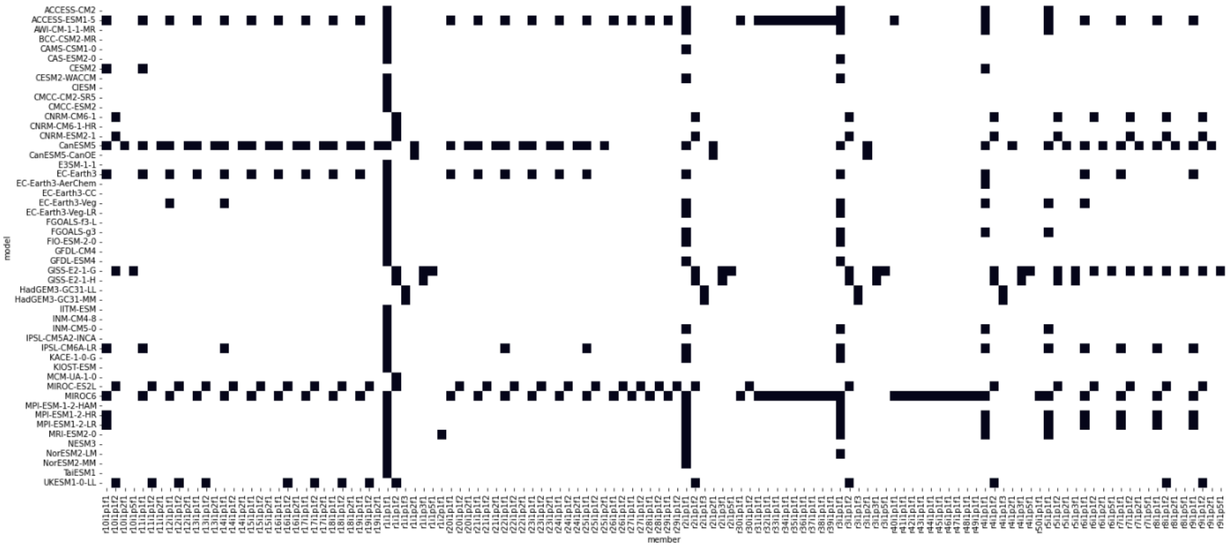

Figure 22. CMIP6 model/member availability based on Google Cloud data.

## 6. Recommended warming year datasets

Based on the preceding discussion and analysis, we recommend the use of warming years from the dataset of 37 models which provide data for every tier 1 scenario, using one member per model, and the four tier 1 scenarios.

Selection of the ‘best’ ensemble member to use for each model is not straightforward in part because member variant IDs (e.g. r1i1p1f1) do not mean the same thing from model to model. After requiring that a member provide data for all tier 1 scenarios for the model of interest, we selected the single member to use for each model based on the following criteria:

1. If r1i1p1f1 is available we used that member
2. If all available members end in i1p1f1, then we selected the lowest numbered realization index
3. If all available members end in f2 and r1i1p1f2 is available, we used that member
4. If all available members include p2 and r1i1p2f1 is available, we used that member
5. For models where the choice was unclear (GISS-E2-1-G and GISS-E2-1-H), we somewhat arbitrarily selected a member, with a preference for lower numbers

### 6.1 Best subset warming year table based on 21 year window approach

Using the above criteria we created a ‘best subset’ table of warming years using the 21 year moving window approach. This dataset is designed to be aggregated across models, members, and/or scenarios. The dataset represents a maximum of 3192 data points (37 models x 4 scenarios x 1 member x 21 years) for each warming level, providing a large sample size that may be useful for analyses concerned with extreme values. Higher warming levels may not be

reached by all model/member/scenario combinations, in which case the sample size would be smaller (see section 6.3). A snapshot of the table is shown in Figure 23. The full table is available upon request and the code for making the table is available in the GitHub repository (make_warming_year_table_for_yr_window_best_subset.ipynb). The table includes warming years for each combination of model/member/scenario and each 0.5°C warming level from 1°C to 4.5°C. NaN values indicate that the warming level was not reached by 2099 for that particular model/member/scenario combination.
The warming year table can be used in combination with the utility functions in the GitHub repository (e.g. get_cmip6_data_at_warming_years()) to easily import data for different CMIP6 variables. For example, the script output_aggregated_warming_level_datasets.ipynb was used to ingest all the warming years included in this table as well as the 10 prior and subsequent years and average across all models, members, scenarios, and years at once for each warming level. The outputs of this script are two netCDF files. One contains mean annual temperature (tas) and the other contains mean annual precipitation, both of which are calculated at each warming level on a 0.5° global grid. These datasets are available upon request.

| | model | member | scenario | Yr1.0 | Yr1.5 | Yr2.0 | Yr2.5 | Yr3.0 | Yr3.5 | Yr4.0 | Yr4.5 |
|---|---|---|---|---|---|---|---|---|---|---|---|
| **3** | GFDL-ESM4 | r1i1p1f1 | ssp126 | 2020.0 | NaN | NaN | NaN | NaN | NaN | NaN | NaN |
| **4** | GFDL-ESM4 | r1i1p1f1 | ssp245 | 2019.0 | 2046.0 | 2073.0 | NaN | NaN | NaN | NaN | NaN |
| **5** | GFDL-ESM4 | r1i1p1f1 | ssp370 | 2022.0 | 2042.0 | 2058.0 | 2070.0 | 2083.0 | NaN | NaN | NaN |
| **6** | GFDL-ESM4 | r1i1p1f1 | ssp585 | 2021.0 | 2040.0 | 2053.0 | 2065.0 | 2076.0 | 2086.0 | NaN | NaN |
| **23** | IPSL-CM6A-LR | r1i1p1f1 | ssp126 | 2003.0 | 2019.0 | 2039.0 | NaN | NaN | NaN | NaN | NaN |
| **...** | ... | ... | ... | ... | ... | ... | ... | ... | ... | ... | ... |
| **1162** | CMCC-ESM2 | r1i1p1f1 | ssp585 | 2004.0 | 2029.0 | 2039.0 | 2048.0 | 2055.0 | 2063.0 | 2070.0 | 2079.0 |
| **1283** | ACCESS-ESM1-5 | r31i1p1f1 | ssp126 | 2015.0 | 2028.0 | NaN | NaN | NaN | NaN | NaN | NaN |
| **1284** | ACCESS-ESM1-5 | r31i1p1f1 | ssp245 | 2013.0 | 2029.0 | 2046.0 | 2064.0 | NaN | NaN | NaN | NaN |
| **1285** | ACCESS-ESM1-5 | r31i1p1f1 | ssp370 | 2014.0 | 2030.0 | 2045.0 | 2060.0 | 2070.0 | 2082.0 | NaN | NaN |
| **1286** | ACCESS-ESM1-5 | r31i1p1f1 | ssp585 | 2013.0 | 2027.0 | 2041.0 | 2052.0 | 2062.0 | 2071.0 | 2081.0 | 2090.0 |

148 rows × 11 columns

Figure 23. Snapshot of the table encompassing the best subset of warming years based on the 21 year moving window approach.

### 6.2 Best subset warming year table based on temperature window approach

Using the same criteria as above for selecting models, members, and scenarios, we developed a series of tables of warming years based on a 0.25°C temperature window (+/-0.25°C either side of the target warming level). Each table contains warming years for a different global warming level (1°C, 1.5°C, 2°C, 2.5°C, 3°C, 3.5°C, 4°C, and 4.5·°C). Model/member/scenario combinations that do not reach the warming level are not included in the table. These tables are available upon request. The files are labeled ‘0.5C window’ (i.e. the size of the full temperature window, not the tolerance either side of the warming level) for consistency with the 21 year

window approach. The code for creating these tables and other warming year tables based on the temperature window approach is available in the GitHub repository (make_warming_year_table_for_temperature_window_best_subset.ipynb). The temperature window tables are organized slightly differently than the 21yr window table presented in section 6.1 since the number of years varies for each model/member/scenario combination. A snapshot of the 4.5°C warming level table is shown in Figure 24.
The script output_aggregated_warming_level_datasets.ipynb was used to ingest all the warming years included in these tables and average across all models, members, scenarios, and years at once for each warming level. The outputs of this script are two netCDF files. One contains mean annual temperature (tas) and the other contains mean annual precipitation, both of which are calculated at each warming level on a 0.5° global grid. These datasets are available upon request.

| | model | member | scenario | year |
|---|---|---|---|---|
| 930 | GFDL-ESM4 | r1i1p1f1 | ssp585 | 2099 |
| 3537 | IPSL-CM6A-LR | r1i1p1f1 | ssp370 | 2082 |
| 3538 | IPSL-CM6A-LR | r1i1p1f1 | ssp370 | 2083 |
| 3539 | IPSL-CM6A-LR | r1i1p1f1 | ssp370 | 2084 |
| 3540 | IPSL-CM6A-LR | r1i1p1f1 | ssp370 | 2085 |
| ... | ... | ... | ... | ... |
| 174610 | ACCESS-ESM1-5 | r31i1p1f1 | ssp585 | 2090 |
| 174611 | ACCESS-ESM1-5 | r31i1p1f1 | ssp585 | 2091 |
| 174612 | ACCESS-ESM1-5 | r31i1p1f1 | ssp585 | 2092 |
| 174614 | ACCESS-ESM1-5 | r31i1p1f1 | ssp585 | 2094 |
| 174615 | ACCESS-ESM1-5 | r31i1p1f1 | ssp585 | 2095 |

407 rows × 4 columns

Figure 24. Snapshot of the warming year table for a warming level of 4.5°C based on the temperature window approach.

### 6.3 Sample sizes for best subset warming year tables

The number of data points (i.e. the sample size) available in the warming year tables from the two methods presented above (sections 6.1 and 6.2) varies by warming level since not all model/member/scenario combinations reach all warming levels. In addition, for the 21 year moving window approach each warming year in the table represents the midpoint of the 21 year period, and therefore 21 data points, whereas each warming year in the temperature window tables represents only one year. Table 4 lists the number of data points (aka sample size; number of warming years across all models, members, and scenarios in the table) available for each approach and for each warming level evaluated. For lower warming levels (2.5°C or less), the two approaches yield similar sample sizes. For higher warming levels (>2.5°C), the 21 year window approach yields consistently larger sample sizes.

| Warming Level | 21 year window approach | 0.25°C temperature window approach |
|---|---|---|
| 1°C | 3108 | 2911 |
| 1.5°C | 3003 | 3047 |
| 2°C | 2730 | 2691 |
| 2.5°C | 2289 | 2187 |
| 3°C | 1848 | 1500 |
| 3.5°C | 1491 | 1013 |
| 4°C | 924 | 652 |
| 4.5°C | 630 | 407 |

Table 4. Number of data points available in the best subset warming year tables for each approach and warming level.

## 7. Data Availability

We are currently in the process of posting the datasets associated with this project to a publicly accessible repository. In the meantime, the datasets are available upon request from the Woodwell Risk Team (contact alute@woodwellclimate.org or cschwalm@woodwellclimate.org).

## 8. Code Availability

Code associated with this project is available on GitHub at https://github.com/WoodwellRisk/Warming_levels.

## 9. References

Caesar, J., Palin, E., Liddicoat, S., Lowe, J., Burke, E., Pardaens, A., Sanderson, M., & Kahana, R. (2013). Response of the HadGEM2 Earth System Model to Future Greenhouse Gas Emissions Pathways to the Year 2300, *Journal of Climate*, *26*(10), 3275-3284. Doi: https://doi.org/10.1175/JCLI-D-12-00577.1.

Deser, C., Lehner, F., Rodgers, K.B. et al. (2020). Insights from Earth system model initial-condition large ensembles and future prospects. Nat. Clim. Chang. 10, 277–286. https://doi.org/10.1038/s41558-020-0731-2

IPCC (2018). Global Warming of 1.5°C. An IPCC Special Report on the impacts of global warming of 1.5°C above pre-industrial levels and related global greenhouse gas emission pathways, in the context of strengthening the global response to the threat of climate change, sustainable development, and efforts to eradicate poverty [Masson-Delmotte, V., P. Zhai, H.-O. Pörtner, D. Roberts, J. Skea, P.R. Shukla, A. Pirani, W. Moufouma-Okia, C. Péan, R. Pidcock, S. Connors, J.B.R. Matthews, Y. Chen, X. Zhou, M.I. Gomis, E. Lonnoy, T. Maycock, M. Tignor, and T. Waterfield (eds.)]. Cambridge University Press, Cambridge, UK and New York, NY, USA, 616 pp., doi: https://doi.org/10.1017/9781009157940.

James, R., Washington, R., Schleussner, C.-F., Rogelj, J. and Conway, D. (2017). Characterizing half-a-degree difference: a review of methods for identifying regional climate responses to global warming targets. WIREs Clim Change, 8: e457. Doi: https://doi.org/10.1002/wcc.457.

Pendergrass, A. G., Lehner, F., Sanderson, B. M., and Xu, Y. (2015). Does extreme precipitation intensity depend on the emissions scenario?, *Geophys. Res. Lett.*, 42, 8767– 8774, doi: https://doi.org/10.1002/2015GL065854.

Seneviratne, S., Donat, M., Pitman, A. *et al.* (2016). Allowable CO2 emissions based on regional and impact-related climate targets. *Nature* 529, 477–483. Doi: https://doi.org/10.1038/nature16542.

Seneviratne, S. I., & Hauser, M. (2020). Regional climate sensitivity of climate extremes in CMIP6 vs CMIP5 multi-model ensembles. Earth's Future. 8, e2019EF001474. Doi: https://doi.org/10.1029/2019EF001474.

Seneviratne, S.I., X. Zhang, M. Adnan, W. Badi, C. Dereczynski, A. Di Luca, S. Ghosh, I. Iskandar, J. Kossin, S. Lewis, F. Otto, I. Pinto, M. Satoh, S.M. Vicente-Serrano, M. Wehner, and B. Zhou, (2021). Weather and Climate Extreme Events in a Changing Climate. In Climate Change 2021: The Physical Science Basis. Contribution of Working Group I to the Sixth Assessment Report of the Intergovernmental Panel on Climate Change [Masson-Delmotte, V., P. Zhai, A. Pirani, S.L. Connors, C. Péan, S. Berger, N. Caud, Y. Chen, L. Goldfarb, M.I. Gomis, M. Huang, K. Leitzell, E. Lonnoy, J.B.R. Matthews, T.K. Maycock, T. Waterfield, O. Yelekçi, R. Yu, and B. Zhou (eds.)]. Cambridge University Press, Cambridge, United Kingdom and New York, NY, USA, pp. 1513–1766, https://www.ipcc.ch/report/ar6/wg1/downloads/report/IPCC_AR6_WGI_Chapter11.pdf.

Tebaldi, Claudia and Knutti, Reto (2007), The use of the multi-model ensemble in probabilistic climate projections. Phil. Trans. R. Soc. A. 365: 2053–2075. doi: http://doi.org/10.1098/rsta.2007.2076.

Tebaldi, C., Debeire, K., Eyring, V., Fischer, E., Fyfe, J., Friedlingstein, P., Knutti, R., Lowe, J., O'Neill, B., Sanderson, B., van Vuuren, D., Riahi, K., Meinshausen, M., Nicholls, Z., Tokarska, K. B., Hurtt, G., Kriegler, E., Lamarque, J.-F., Meehl, G., Moss, R., Bauer, S. E., Boucher, O., Brovkin, V., Byun, Y.-H., Dix, M., Gualdi, S., Guo, H., John, J. G., Kharin, S., Kim, Y., Koshiro, T., Ma, L., Olivié, D., Panickal, S., Qiao, F., Rong, X., Rosenbloom, N., Schupfner, M., Séférian, R., Sellar, A., Semmler, T., Shi, X., Song, Z., Steger, C., Stouffer, R., Swart, N., Tachiiri, K., Tang, Q., Tatebe, H., Voldoire, A., Volodin, E., Wyser, K., Xin, X., Yang, S., Yu, Y., and Ziehn, T. (2021). Climate model projections from the Scenario Model Intercomparison Project (ScenarioMIP) of CMIP6, Earth Syst. Dynam., 12, 253–293, doi: https://doi.org/10.5194/esd-12-253-2021.

UNFCCC (2015). Adoption of the Paris Agreement. See http://unfccc.int/resource/docs/2015/cop21/eng/l09r01.pdf.

Wartenburger, R., Hirschi, M., Donat, M. G., Greve, P., Pitman, A. J., and Seneviratne, S. I. (2017). Changes in regional climate extremes as a function of global mean temperature: an interactive plotting framework, Geosci. Model Dev., 10, 3609–3634, doi: https://doi.org/10.5194/gmd-10-3609-2017.